Juvenile Cataract-Associated Mutation of Solute Carrier *SLC16A12* Impairs Trafficking of the Protein to the Plasma Membrane

John J. Castorino,[1] Shannon M. Gallagher-Colombo,[1] Alex V. Levin,[2] Paul G. FitzGerald,[3] Jessica Polishook,[1] Barbara Kloeckener-Gruissem,[4,5] Eric Ostertag,[6,7,8] and Nancy J. Philp[1]

Purpose. *SLC16A12* encodes an orphan member of the monocarboxylate transporter family, MCT12. A nonsense mutation in *SLC16A12* (c.643C>T; p.Q215X) causes juvenile cataract with a dominant inheritance pattern. In the present study, in vitro and in vivo experimental models were used to gain insight into how the *SLC16A12* (c.643C>T) mutation leads to cataract formation.

Methods. MCT12 peptide antibodies were generated and used to examine the expression of MCT12 in the lens using immunoconfocal microscopy. To determine whether loss of *Slc16a12* resulted in cataract formation, a *Slc16a12* hypomorphic rat generated by transposon insertional mutagenesis was characterized using RT-PCR, slit lamp microscopy and histologic methods. Exogenous expression of MCT12 and MCT12:214Δ, a mimic of the mutant allele, were used to assess protein expression and trafficking.

Results. MCT12 protein was detected in the lens epithelium and secondary fiber cells at postnatal day 1. In the *Slc16a12^{TKO}* rat, complete loss of MCT12 did not result in any detectable ocular phenotype. Exogenous expression of MCT12-GFP and MCT12:214Δ-GFP revealed that the full-length protein was trafficked to the plasma membrane (PM), whereas the truncated protein was retained in the endoplasmic reticulum (ER). When both MCT12 and MCT12:214Δ were coexpressed, to mimic the heterozygous patient genotype, the truncated protein was retained in the ER whereas full-length MCT12 was trafficked to the PM. Furthermore, MCT12 was identified as another MCT isoform that requires CD147 for trafficking to the cell surface.

Conclusions. These data support a model whereby the *SLC16A12* (c.643C>T) mutation causes juvenile cataract by a defect in protein trafficking rather than by haploinsufficiency. (*Invest Ophthalmol Vis Sci.* 2011;52:6774–6784) DOI:10.1167/iovs.10-6579

Recently, it was reported that a mutation in the *SLC16A12* gene that encodes the solute transporter MCT12 was linked to autosomal dominant juvenile lens cataract.[1] Patients with the c.643C>T; p.Q215X mutation presented with corticonuclear cataract, microcornea, and renal glucosuria.[1] *SLC16A12* is an orphan member of the monocarboxylate transporter (MCT) gene family (*SLC16*). Fourteen members in the *SLC16A* gene family have been identified, and the different MCT isoforms vary in their substrate specificity and tissue distribution. MCT1 to MCT4 transport lactate and other monocarboxylic acids,[2,3] MCT8 transports thyroid hormone,[4] MCT9 has been reported to function as a carnitine or urate transporter,[5,6] and MCT10 transports aromatic amino acids.[7,8] The natural substrate specificities of the other members of the MCT family, including MCT12, have not yet been determined. MCT12 shares the greatest amino acid sequence identity with MCT4 (31%) and MCT3 (30%), but some residues critical for lactate transport are not conserved.[2,9] Therefore, it is not possible to predict the substrate specificity of MCT12 based solely on sequence homology.

MCTs, like other solute transporters, have twelve membrane spanning domains and the amino and carboxy termini are cytoplasmic. With the exception of the intracellular loop between the sixth and seventh transmembrane domains, the intracellular and extracellular loops are relatively short. MCT1 to MCT4 are functional heterodimers and require an accessory protein for their maturation and trafficking from the endoplasmic reticulum (ER) to the plasma membrane.[10–13] CD147 is the accessory protein for MCT1, MCT3, and MCT4,[10,12] whereas embigin is the accessory protein for MCT2.[14] It is not yet known whether other members of the *SLC16* family, including MCT12, require CD147 for trafficking to the plasma membrane.

Based on the predicted secondary structure of MCT12, the c.643C>T; p.Q215X mutation in *SLC16A12* would be expected to encode a protein with only the first six transmembrane domains given that Q215 is found in the large intracellular loop between the sixth and seventh transmembrane domains.[1] Based on the predicted tertiary structure of other MCTs, the mutant protein would not produce a functional transporter, and folding and trafficking of the mutant protein would likely be impaired. In patients carrying the mutant *SLC16A12* gene, cataract formation could be caused by haploinsufficiency. Alternatively, misfolding of the mutant protein

From the [1]Department of Pathology, Anatomy, and Cell Biology, Jefferson Medical College, Thomas Jefferson University, Philadelphia, Pennsylvania; [2]Department of Ophthalmology and Ocular Genetics, Wills Eye Institute, Philadelphia, Pennsylvania; [3]Department of Cell Biology and Human Anatomy, School of Medicine, University of California, Davis, California; [4]Institute of Medical Molecular Genetics, University of Zurich, Zurich, Switzerland; [5]Department of Biology, ETHZ, Zurich, Switzerland; [6]Transposagen Biopharmaceuticals, Inc., Lexington, Kentucky; [7]Department of Microbiology, Immunology, and Molecular Genetics, University of Kentucky, Lexington, Kentucky; and [8]Department of Pathology and Laboratory Medicine, University of Kentucky Chandler Hospital, Lexington, Kentucky.

Supported by National Institutes of Health Grants EY012042 (NJP) and EY08747 (PGF).

Submitted for publication September 15, 2010; revised February 9, June 13, and July 7, 2011; accepted July 11, 2011.

Disclosure: **J.J. Castorino**, None; **S.M. Gallagher-Colombo**, None; **A.V. Levin**, None; **P.G. FitzGerald**, None; **J. Polishook**, None; **B. Kloeckener-Gruissem**, None; **E. Ostertag**, None; **N.J. Philp**, None

Corresponding author: Nancy J. Philp, Department of Pathology, Anatomy, and Cell Biology, Jefferson Medical College, Thomas Jefferson University, 1020 Locust Street, Philadelphia, PA 19107; nancy.philp@jefferson.edu.

could cause cataract formation, as has been reported for cataract-associated mutations in connexins and crystallins.[15]

In the present study, we used in vitro and in vivo experimental models to gain insight into how the *SLC16A12*(c.643C>T) mutation may cause cataracts by testing two possible mechanisms, haploinsufficiency and protein misfolding. Exogenous expression of full-length and truncated MCT12 proteins in HEK-293 cells revealed that the full-length MCT12 was trafficked to the plasma membrane while the truncated MCT12 was retained in the ER. Furthermore, in the *Slc16a12*^{TKO} rat, complete loss of MCT12 did not result in any detectable ocular phenotype. From these studies, we propose that the dominant form of cataract observed in patients harboring the *SLC16A12* mutation most likely results from a defect in folding and trafficking of the mutant protein rather than from haploinsufficiency.

METHODS

Chemicals

All reagents were purchased from Sigma Chemical Co. (St. Louis, MO) unless otherwise stated.

Animals

Mice (C57BL/6) were obtained from Charles Rivers Laboratories (Wilmington, MA). Fischer (F344) rat strains used in these studies were provided by Transposagen Biopharmaceuticals, Inc. (Lexington, KY). All animals were maintained on a 12-hour light/12-hour dark cycle. The animals were killed during the light period of the cycle. All animal procedures were performed in compliance with National Institutes of Health guidelines as approved by the Institutional Animal Care and Use Committee of Thomas Jefferson University. Procedures are in accordance with the ARVO Statement for the Use of Animals in Ophthalmic and Vision Research.

Genetic modification of *Rattus norvegicus* gene solute carrier family 16, member 12 (*Slc16a12*) was carried out by DNA transposon insertional mutagenesis using a gene trap, as described previously.[16] The DNA transposon-modified allele was designated Slc16a12Tn(sb-T2/Bart3)2.298Mcwi. The Rat Genome Database mutant strain symbol for the genetically modified rat was designated F344-Slc16a12Tn(sb-T2/Bart3)2.298Mcwi. The insertion site of the transposon is intronic, between the first and second coding exons of the *Slc16a12* gene located on chromosome 1 in the Fischer (F344) rat strain. The genomic DNA flanking the 5′ end of the insertion is TACGTCCTCATGTATTAACTTTGGTCAA-TATGGAATTAAGATAAGATTGGCAGTGAGACAAATTCAGGCCTGGATAG-TTAGGGCTGGCTTTCTAG. Additional information about this rat model can be found at the Transposagen Biopharmaceuticals, Inc. Web site (www.transposagen.com).

Genotyping

Genomic DNA was prepared from ear clippings and analyzed by PCR. PCR conditions were as follows: 94°C, 7 minutes; (94°C, 30 seconds; 58°C, 30 seconds; 72°C, 45 seconds) × 40 cycles; 72°C, 7 minutes. Wild-type (1031 bp) and knockout (594 bp) amplicons were generated with the primer sets shown in Supplementary Table S1, http://www.iovs.org/lookup/suppl/doi:10.1167/iovs.10-6579/-/DCSupplemental. PCR products were separated on 1.5% agarose gels. Rats with only the wild-type locus, one copy of the transposon and two copies of the transposon are referred to as *Slc16a12*^{WT}, *Slc16a12*^{bet}, and *Slc16a12*^{TKO}, respectively.

RT-PCR

Total RNA was extracted from cells using purification kits (RNeasy Mini; Qiagen, Valencia, CA) according to the manufacturer's protocol. cDNA was synthesized from 300 ng total tissue RNA or 2 μg cell-extracted RNA by reverse transcriptase (SuperScript III; Invitrogen, Carlsbad, CA) with oligo dT primers. PCR was performed with 1 μL cDNA with the primers and conditions described in Supplementary Table S2, http://www.iovs.org/lookup/suppl/doi:10.1167/iovs.10-6579/-/DCSupplemental, and Fisher *Taq* polymerase. Expression of *Slc16a12* in rat tissues and human cell lines was determined by RT-PCR. PCR products were separated on 1.5% agarose gels.

Generation of MCT12 Expression Vectors

Full-length MCT12 was amplified from cDNA prepared from human fetal retinal pigment epithelial cells with the forward primer gcgaactc-gagccaccatggcaaaagtaaatagagctc (which includes an *Xho*I site) and the reverse primer gcgaagaattcctgtgaggctgtagccagg (which includes an *Eco*RI site). MCT12:214Δ was amplified with the same forward primer but with the reverse primer gcgaagaattccagttctacacacatggttctgc (which also includes an *Eco*RI site). PCR products were digested with *Xho*I and *Eco*RI and were cloned into these sites of the pEGFP-N1 or pmCherry-C1 vectors (Clontech, Mountain View, CA). All constructs were confirmed to be free of mutations by sequencing at the Thomas Jefferson University Nucleic Acid Facility.

Cell Culture and Transfection

HEK-293 and HLE-B3 cells (generously provided by Dwight Stambolian) were cultured in Dulbecco's modified Eagle's medium containing 1% penicillin/streptomycin, 2 mM glutamine, and 5% fetal bovine serum in a humidified atmosphere of 5% CO_2 at 37°C. Cells were transfected with vectors expressing MCT12-GFP, MCT12:214Δ-GFP, mCherry-MCT12, or mCherry-MCT12:214Δ using transfection reagent (Fugene-6; Roche, Indianapolis, IN) in accordance with the manufacturer's instructions. All tissue culture vessels were poly lysine–coated before plating. When required, stable cell lines were generated by selection with aminoglycoside antibiotic (0.8 mg/mL G418; Mediatech, Manassas, VA). Non-clonally derived stable cell lines expressing MCT12-GFP are referred to as HEK-293:MCT12-GFP cells. We were unable to derive stable lines of cells expressing MCT12:214Δ.

Antibodies

Anti–peptide antibodies were raised in rabbits against the synthetic oligopeptide SDPKLQLWTNGSVAYSVARELDQ corresponding to the amino acids 478 to 500 within the C-terminal cytoplasmic tail of human MCT12 (Yenzym, Inc., San Francisco, CA). Antibody specificity was confirmed with immunostaining of cells transiently transfected with MCT12-GFP, which showed that only cells expressing the fusion were labeled with the antibody (see Fig. 2B). Anti–peptide antibodies to MCT1 were generated as previously described.[17] Additional antibodies used in these studies were anti–human CD147 (for immunoprecipitation; Fitzgerald Industries International, Acton, MA), anti–human CD147 (for Western blot, N19; Santa Cruz Biotechnology, Santa Cruz, CA), anti–GRP78 (for immunofluorescence; Sigma), anti–β-actin and anti–GFP (anti–rabbit for immunoprecipitation and anti–goat for Western blot; Rockland Immunochemicals, Inc., Gilbertsville, PA). Alexa Fluor and horseradish peroxidase (HRP)–conjugated secondary antibodies were purchased from Invitrogen and Thermo Fisher Scientific, respectively.

Immunofluorescence

Cells grown on poly lysine–coated two-well chamber slides were fixed in 4% paraformaldehyde (Electron Microscopy Sciences, Hatfield, PA) in PBS for 5 minutes at room temperature, followed by 25 minutes on ice. Cells were washed in PBS, permeabilized with methanol for 3 minutes at −20°C, blocked using 5% BSA in PBS with 0.1% Tween 20 (PBST), and incubated with primary antibody overnight at 4°C. The next day, cells were washed with PBST and incubated in secondary antibody for 30 minutes, washed, and mounted with mounting medium (Gelvatol; Sigma). Antibodies were used at the following dilutions: MCT12 (rabbit, 1:200) donkey anti–rabbit IgG-Alexa-Fluor 555 (rabbit, 1:500). Images were processed with fluorescent protein imaging software (LSM 510; Zeiss, Thornwood, NY) and image-editing

software (Photoshop 7.0; Adobe, San Jose, CA). Adjustments were made to brightness and contrast only.

For tissue sections, animals were euthanized by overdose of anesthetic followed by cardiac perfusion with 4% paraformaldehyde in PBS. Tissues were removed, washed in PBS, and cryoprotected by with 30% sucrose/PBS before they were embedded in OCT compound (Tissue-Tek; Sakura Finetek, Torrance, CA). Cryosections (8–10 μm) were cut and collected on glass slides (Superfrost; Fisher Scientific, Inc.). Sections were rehydrated and then blocked and labeled with antibodies as described.

Immunoprecipitation

Cells were washed twice with PBS and lysed with ice-cold CHAPS lysis buffer (25 mM HEPES buffer, pH 7.4, 150 mM NaCl, 5 mM $MgCl_2$, 1% CHAPS detergent) containing protease inhibitors for 30 minutes. The lysate was clarified by centrifugation at 14,000*g* for 30 minutes. An aliquot of the supernatant was removed for protein analysis, and 1 mg supernatant was incubated with 1 μL anti–GFP, 2 μL anti–MCT12, or 1 μL anti–CD147 antibody overnight with end-over rotation at 4°C. The following day, 20 μL immobilized protein A/G plus beads (ImmunoPure; Pierce, Rockford, IL) were added, and the samples were incubated for 4 hours with end-over rotation at 4°C. Cell lysates were also incubated with beads only (no antibody added) as a control. The beads were washed three times with lysis buffer. Bound proteins were eluted from the beads with 2× lithium dodecyl sulfate (LDS) sample buffer, and proteins were analyzed by SDS-PAGE and immunoblotting. Immunoprecipitation experiments were performed at least three times for each condition. Similar results were obtained in all experiments.

Biotinylation of Cell Surface Proteins

Cells were washed with PBS and then incubated with 0.5 mg/mL biotinylation reagent (EZ Link Sulfo-NHS-LC-Biotin; Pierce) in PBS for 30 minutes at room temperature. After 30 minutes, the reaction was quenched by washing the plates three times with PBS containing 100 mM glycine. Cells were extracted in ice-cold Triton lysis buffer (25 mM HEPES buffer, pH 7.4, 150 mM NaCl, 5 mM $MgCl_2$, 1% Triton X-100, 60 mM n-octyl-glucopyranoside) containing protease inhibitors. An aliquot of the cleared lysates was removed for protein determination, and another aliquot was diluted 1:1 with 2× LDS sample buffer (Invitrogen) for analysis of biotinylated proteins by SDS-PAGE. One milligram of soluble protein was incubated overnight with rotating at 4°C with streptavidin-agarose beads (Thermo Scientific) at 4°C with end-over rotation. Beads were washed three times with lysis buffer, and precipitated proteins were eluted with 50 μL 2× LDS sample buffer.

siRNA-Mediated Knockdown

HEK-293 cells stably expressing MCT12-GFP were transfected with CD147-specific or control siRNA characterized previously using an electroporator (Neon; Invitrogen).[13] Briefly, cells were trypsinized, washed twice in PBS, and resuspended in resuspension buffer (Invitrogen) to achieve 3×10^5 cells and 0.5 μL 10μM siRNA per 10 μL transfection. Cells were pulsed twice at 1200 V for 20 ms each; 60-mm dishes received two sets of electroporated cells each, whereas two-well chamber slides received one set of electroporated cells.

Immunoblot Analysis

Detergent-soluble lysates were diluted in 2× LDS sample buffer (Invitrogen), and protein samples were resolved on 4% to 12% Bis-Tris gels (NuPAGE; Invitrogen) and transferred to membranes (Immobilon-P; Millipore, Bedford, MA). Membranes were incubated for 1 hour at room temperature in blocking buffer (20 mM Tris, 137 mM NaCl, pH 7.5, 5% dry skim milk), followed by 1-hour incubation with primary antibodies and 30-minute incubation with HRP-conjugated secondary antibodies diluted 1:5000. Blots were probed with the following antibodies: MCT1 (1:1000), CD147 (1:1000), and GFP (goat, 1:1000). β-Actin (mouse, 1:50,000) was used as a loading control. Reactive bands were visualized with enhanced chemiluminescence Western blotting detection reagents (Pierce) and x-ray film. Films were scanned (Perfection 3200; Epson, Long Beach, CA), and densitometry measurements were performed on resultant tiff images (AlphaEaseFC software and the Spot Denso tool, version 4.0.0; Alpha Innotech, San Leandro, CA).

Imaging of Rat Eyes

Both eyes from 2- and 4-month-old rats were dilated by applying 1 to 2 drops of 1% tropicamide solution to each eye approximately 15 minutes before examination using a portable slit lamp biomicroscope. Observations of lens clarity and any other anterior segment findings in each eye were manually recorded. In addition, the eyes of the animals were imaged using a camera (Lumix; Panasonic, Newark, NJ) to display gross morphology of the eye in addition to clarity of the lens. Images were processed with image editing software (Photoshop 7.0; Adobe). To further determine lens clarity, lenses were removed from eyes of 7- to 10-week-old rats and placed on 300 mesh square copper grids (Electron Microscopy Sciences). Lenses were imaged using a microscope (Eclipse E800; Nikon, Tokyo, Japan) under the 4× objective. Images were obtained using an digital camera (Optronics, Wake Forest, NC) and were processed using image analysis software (BioQuant [Bioquant Image Analysis Corp., Nashville, TN] and Photoshop 7.0 [Adobe]).

Histology

After slit lamp examination, 8- to 10-week-old *Slc16a12*^{WT}, *Slc16a12*^{bet} and *Slc16a12*^{TKO} rats were euthanized, and eyes were removed and fixed for histologic analysis. Briefly, each animal received a lethal dose of barbiturate and was then perfused with 50 to 100 mL of a 2.5% paraformaldehyde/0.25% glutaraldehyde solution. After perfusion, eyes were removed and placed in 4% paraformaldehyde for 24 hours. Eyes were prepared for paraffin sectioning either by the Histology Core Facility in the Kimmel Cancer Center at Thomas Jefferson University (Philadelphia, PA) or by Am Histolabs, Inc. (Gaithersburg, MD). These facilities also sectioned the eyes and stained them with hematoxylin and eosin. Sections were examined on a microscope (Eclipse E800; Nikon). Images were obtained with a digital camera (Optronics) and processed using image analysis software (BioQuant [Bioquant Image Analysis Corp.] and Photoshop 7.0 [Adobe]). Adjustments were made to brightness and contrast only.

Scanning Electron Microscopy

Eyes were enucleated, and lenses were removed to 0.1 M cacodylate buffer, pH 7.5, with 2% glutaraldehyde and 2.5% formaldehyde at room temperature. After 1 hour, lenses were bisected and then allowed to continue fixation for 48 hours. Tissues were dehydrated through acetone and critical point dried. Lenses were then split into quarters along the anterior-posterior axis, yielding a freshly fractured surface that exposed a complete lens radius. Specimens were sputter coated before examination with a scanning electron microscope (XL 30; Philips, Andover, MA).

Results

MCT12 Is a Heteromeric Transporter and Requires CD147 for Maturation and Trafficking to the Plasma Membrane

MCT12 is an orphan member of the *SLC16A* family, and, though tissue distribution of the mRNA has been reported, nothing is known about the expression, trafficking, or function of MCT12 protein. We generated a MCT12-GFP fusion construct and stably expressed it in HEK-293 cells to determine the subcellular distribution of MCT12. Confocal imaging of the cells revealed that MCT12-GFP was predominantly detected in

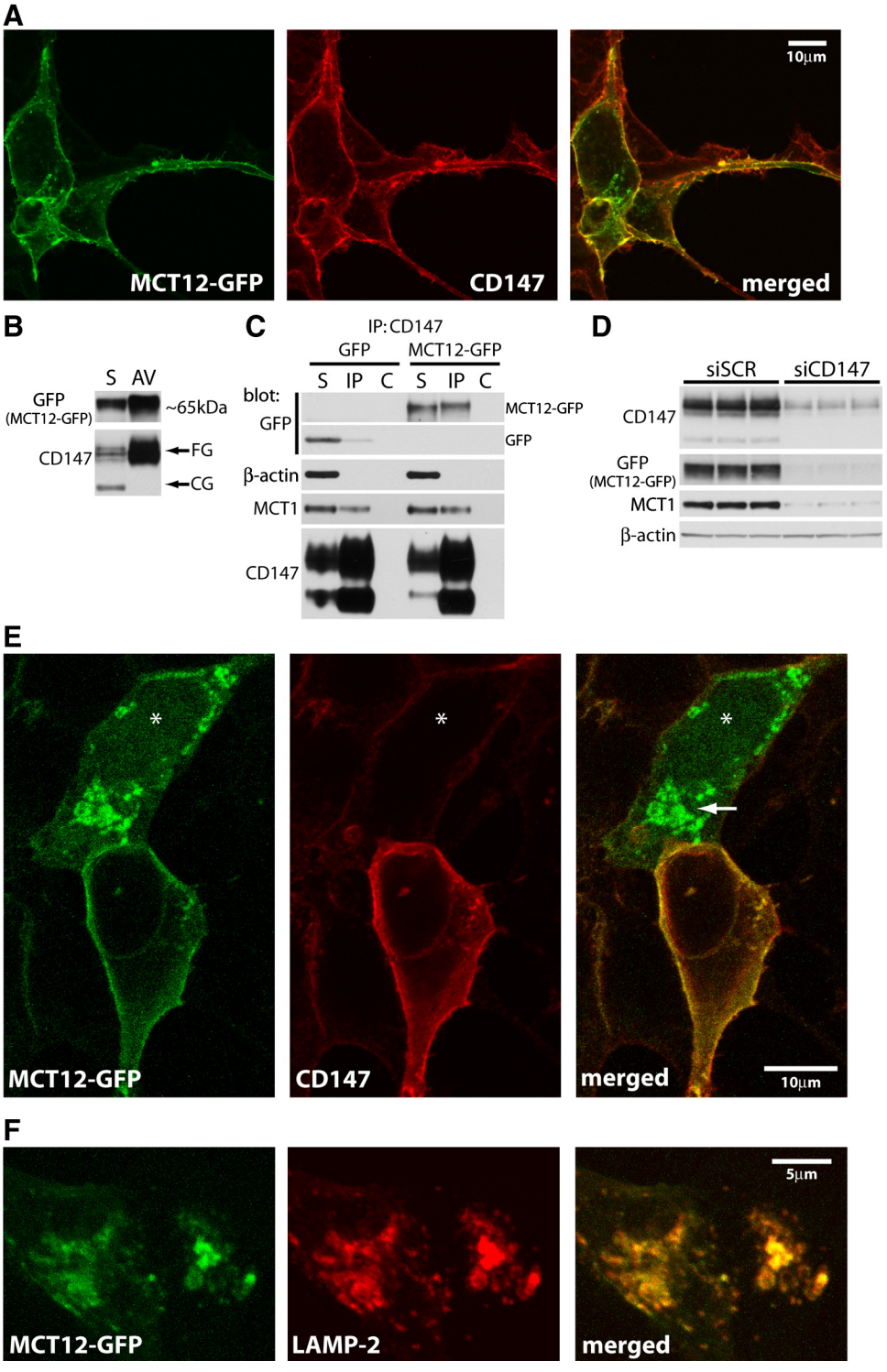

Figure 1. MCT12 is a heteromeric transporter. (**A**) HEK-293:MCT12-GFP cells (*left*) were fixed and immunostained for CD147 (*middle*) to determine whether the proteins colocalize (merged, *right*). (**B**) To confirm MCT12-GFP expression at the plasma membrane, cell-surface biotinylation followed by avidin precipitation was performed on HEK-293:MCT12-GFP cells. Western blot analysis of Triton-soluble cell lysates (10 μg) (S) and avidin-precipitated fractions (Av) were probed for GFP to detect MCT12-GFP and CD147. (**C**) HEK-293:MCT12-GFP cells were extracted in CHAPS buffer, and lysates were immunoprecipitated with CD147 antibody. Soluble lysates (10 μg) (S) and precipitated proteins (immunoprecipitate) were run on PAGE and subjected to Western blot analysis. Lysates were incubated with protein A/G beads alone to confirm the specificity of immunoprecipitate (C). Blots were probed for GFP to determine whether MCT12-GFP precipitated with CD147 and β-actin as a negative control. Blots were probed with MCT1 to show equal precipitation between cell lines. (**D**) HEK-293:MCT12-GFP cells were transfected with siRNA specific for CD147, and Western blots of lysates (10 μg) extracted 72 hours after transfection were probed with CD147, GFP, MCT1, and β-actin antibodies. (**E**) Cells were fixed 24 hours after transfection and immunostained for CD147. *Arrow*: cell in which CD147 has been knocked down. (**F**) Higher power view of intracellular MCT12-GFP vesicles costained with LAMP-2 antibody (*red*).

the plasma membrane, where it colocalized with CD147, the accessory protein for MCT1 (Fig. 1A). The localization of both proteins in the plasma membrane was confirmed by cell-surface biotinylation, followed by avidin precipitation and immunoblot analysis. Both MCT12-GFP and fully glycosylated CD147 were enriched in the avidin pull-down fraction (Fig. 2B). As expected, the core-glycosylated form of CD147 was not biotinylated because this immature form of CD147 is found only in the ER.

To determine whether MCT12 formed a heteromeric complex with CD147, we performed coimmunoprecipitation experiments. Detergent-soluble lysates were prepared from HEK-293 cells stably expressing either GFP alone or MCT12-GFP. Lysates were immunoprecipitated with anti–CD147 antibody, and blots were probed with anti–GFP antibody (Fig. 1C). Blots were also probed with anti–MCT1 antibody as a positive control because it was previously shown that MCT1 forms a heterocomplex with CD147.[10,12] The results showed that MCT12-GFP, like MCT1, coimmunoprecipitates with CD147. We did detect some GFP nonspecifically precipitating with CD147, but the amount of coimmunoprecipitation was substantially lower than with MCT12-GFP or MCT1. To confirm the inter-

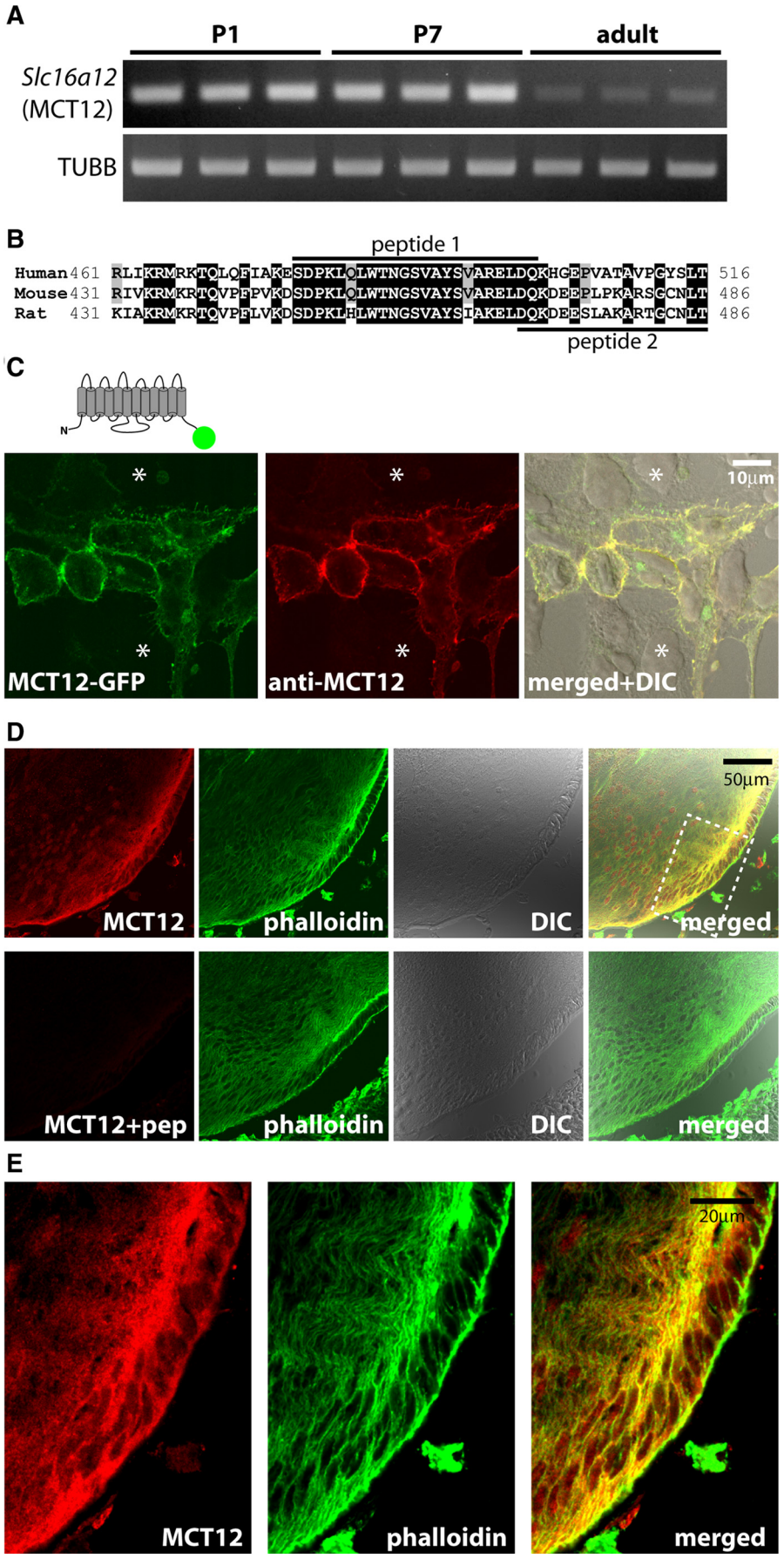

FIGURE 2. Expression of MCT12 in the lens. (**A**) cDNA was prepared from RNA extracted from P1, P7, and 3-month-old (adult) lenses, and PCR was performed for *Slc16a12* and β-tubulin as a loading control. (**B**) Antipeptide antibodies were generated against two regions of the C-terminal cytoplasmic tail. The sequence shown as peptide 1 was used for these studies. Antibodies raised to peptide 2 did not specifically label MCT12 for immunostaining or Western blotting. (**C**) HEK-293 cells transiently transfected with vectors expressing MCT12-GFP were stained with anti–peptide MCT12 antibody (*red*) to confirm antibody specificity. Untransfected cells (*asterisks*) were not labeled by the antibody. (**D**) Frozen tissue sections of P1 mouse lenses were stained with the antipeptide antibody (*red*). Differential interference contrast (DIC) and phalloidin (*green*) show tissue structure. Blocking the antibody with the immunogenic peptide before staining (**D**, lower) prevented all staining. (**E**) Enlargement of the *boxed region* in **D**.

action, the reciprocal coimmunoprecipitate was performed with anti–GFP antibody, followed by Western blot analysis with anti–CD147 antibody. CD147 was confirmed to coimmunoprecipitate with MCT12-GFP (Supplementary Fig. S1A, http://www.iovs.org/lookup/suppl/doi:10.1167/iovs.10-6579/-/DCSupplemental).

To assess whether MCT12 required CD147 for trafficking to the plasma membrane, CD147 was knocked down in HEK-293:MCT12-GFP cells using siRNA. HEK-293:MCT12-GFP cells transfected with either scrambled or CD147-specific siRNA were harvested 72 hours after transfection, and levels of CD147 and MCT12-GFP protein were determined by immunoblot analysis. Silencing of CD147 reduced the levels of MCT12-GFP compared with scrambled siRNA-treated cells (Fig. 1D). As expected, the level of expression of MCT1 was also reduced by silencing CD147, as previously reported.[12,18] Confocal immunofluorescence analysis showed that 24 hours after silencing CD147 in cells in which GFP fluorescence could still be detected, MCT12-GFP was localized to intracellular vesicles (Fig. 1E, arrow). These vesicles colabeled with anti–LAMP-2 antibody, indicating that in the absence of CD147, MCT12-GFP was degraded by the lysosomal pathway (Fig. 1F).

MCT12 Is Expressed in the Lens

To begin to understand how mutations in *SLC16A12* could lead to juvenile cataract, we examined the developmental expression of the *Slc16a12* transcript in postnatal lenses of mice. RT-PCR revealed that *Slc16a12* mRNA was expressed in the lens at postnatal day (P)1 and P7 at higher levels than observed in the adult lens (Fig. 2A).

To examine the spatial distribution of MCT12 protein in the lens, we generated an anti–MCT12 peptide antibody to a highly conserved domain of the C-terminal cytoplasmic tail of MCT12 (Fig. 2B). To validate the antibody specificity, HEK-293 cells expressing MCT12-GFP fusion protein were fixed and labeled with the anti–MCT12 antibody. Immunofluorescence confocal microscopy showed that the anti–MCT12 antibody labeled only cells expressing the MCT12-GFP fusion protein but not untransfected cells (Fig. 2C).

Next we labeled frozen sections of eyes from P1 mouse pups with the anti–MCT12 antibody. MCT12 was detected in the basolateral membrane of the lens epithelium (Fig. 2D), with strongest staining observed at the equatorial epithelium (Supplementary Fig. S1B, http://www.iovs.org/lookup/suppl/doi:10.1167/iovs.10-6579/-/DCSupplemental). Additionally, we observed staining in the differentiating secondary fiber cells of P1 mouse lenses (Figs. 2D, 2E).

Generation of *Slc16a12^{TKO}* Rats

One potential explanation for dominant cataract formation in patients with the *SLC16A12* exon 6:c643C>T mutation could be haploinsufficiency. To address whether this could be the underlying cause for juvenile cataract found in patients, we obtained the *Slc16a12^{TKO}* rat, a functional knockout generated by transposon insertional mutagenesis (Fig. 3A). Heterozygotes were crossed to obtain *Slc16a12^{WT}*, *Slc16a12^{het}* and *Slc16a12^{TKO}* animals, and genotypes of the rats were determined by PCR using primers specific for the wild-type and transposon-inserted loci (Fig. 3B). Rat offspring were born to expected Mendelian genotype ratios, and no obvious phenotypic changes were observed in the transgenic animals even though *Slc16a12* mRNA was detected in a number of ocular tissues (Supplementary Fig. S1C, http://www.iovs.org/lookup/suppl/doi:10.1167/iovs.10-6579/-/DCSupplemental) and organs (Supplementary Fig. S1D, http://www.iovs.org/lookup/suppl/doi:10.1167/iovs.10-6579/-/DCSupplemental) in wild-type rats.

With a focus on cataract formation in these animals, we specifically examined the expression of *Slc16a12* mRNA extracted from whole lenses of adult *Slc16a12^{WT}* and *Slc16a12^{TKO}* animals. To determine that the gene trap was functional, we performed a number of different PCR reactions on cDNA prepared from rat lens mRNA to determine whether *Slc16a12* mRNA was expressed in *Slc16a12^{TKO}* rats (Fig. 3C). Using forward and reverse primers within exon 2 confirmed that the *Slc16a12* locus was transcribed in both the *Slc16a12^{WT}* and *Slc16a12^{TKO}* rats (Fig. 3D). PCR reactions from cDNA prepared without reverse transcriptase generated no products. When primers from exon 2 (forward) and exon 7 (reverse) were used, a product was detected only in wild-type animals, demonstrating the transposon did indeed disrupt normal *Slc16a12* mRNA expression and confirming that the

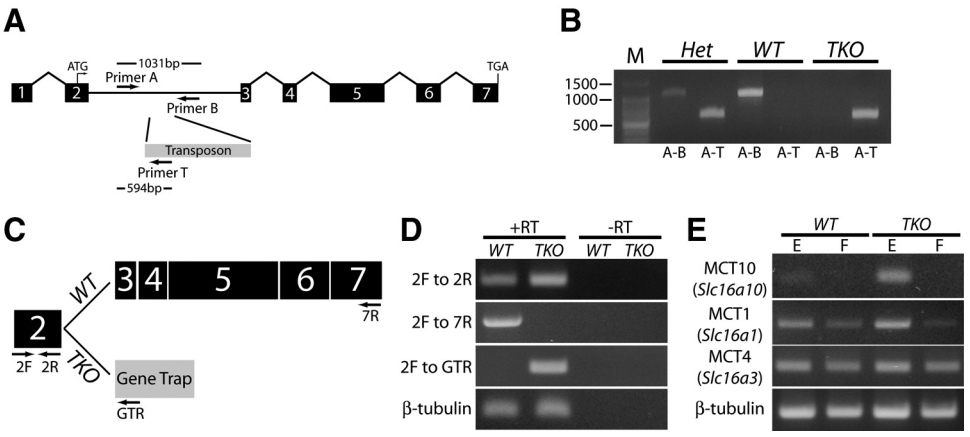

FIGURE 3. Generation of *Slc16a12^{TKO}* rats. (**A**) Schematic of the transposon insertion is presented. Primer set A/B amplifies the wild-type gene, whereas primer set A/T amplifies the knockout fragment of the gene (primer sequences provided in Table S1). Note that the human *SLC16A12* locus has an additional upstream exon that does not seem to be present in the mouse or rat genes. (**B**) Total genomic DNA was analyzed by PCR to determine genotypes of animals used for these studies. Primers A/B yielded a 1031-bp band if the normal *Slc16a12* gene was present (indicative of wild-type). Primers A/T yielded a 594-bp band if only the transposon was present in the *Slc16a12* gene (indicative of the knockout phenotype). Heterozygous animals (het) showed both the 1031-bp and 594-bp bands, whereas the wild-type (WT) showed only the 1031-bp band and the knockout (TKO) showed only the 594-bp band. M, size marker. (**C**) Primers were designed to assess the mRNA generated from *Slc16a12^{WT}* and *Slc16a12^{TKO}* animals. (**D**) cDNA was generated from total DNase-treated RNA extracted from *Slc16a12^{WT}* and *Slc16a12^{TKO}* whole lenses. PCR was performed within rat *Slc16a12* exon 2 to show the locus was transcribed in both genotypes. PCR was performed from exon 2 to exon 7 to show that normal *Slc16a12* mRNA was processed only in *Slc16a12^{WT}* animals and from exon 2 to the gene trap to show that only the mutant mRNA was generated in *Slc16a12^{TKO}* animals. β-Tubulin was amplified as a loading control. No PCR products were produced in samples in which the cDNA reaction did not contain reverse transcriptase (RT). (**E**) PCR was performed for all members of the *Slc16a* family (primer sequences provided in Table S2) on cDNA prepared from microdissected lens epithelium (E) or fiber (F) cells, but only three members in addition to *Slc16a12* were detected. Representative reactions from three different rats are shown.

Slc16a12^{TKO} animals were effectively null. No additional products were amplified in the PCR reactions from animals harboring the transposon that would be indicative of aberrant splicing. PCR using primers from exon 2 and the gene trap amplified a product using only RNA prepared from *Slc16a12*^{TKO} animals, which indicated that the mutated mRNA was expressed. Amplification of β-actin mRNA was used as a loading control in these experiments. Together, these data indicate that the first coding exon is transcribed and that the first 36 amino acids of the MCT12 might be translated, but additional expression of MCT12 protein from the locus in *Slc16a12*^{TKO} rats is unlikely.

Of the 13 additional members of the *Slc16a* gene family, only the mRNA for *Slc16a1*, *Slc16a3*, and *Slc16a10* was detected in the lenses of the *Slc16a12*^{WT} and *Slc16a12*^{TKO} rats (Fig. 3E). The amounts of *Slc16a1* (MCT1) and *Slc16a3* (MCT4) seemed comparable between wild-type and knockout siblings. However, we detected the *Slc16a10* (MCT10) PCR product in the lens epithelium isolated from *Slc16a12*^{TKO} rats but not in age-matched, wild-type siblings.

Slc16a12^{TKO} Rats Do Not Develop Cataracts

Eyes from *Slc16a12*^{WT}, *Slc16a12*^{bet}, *and Slc16a12*^{TKO} rats at 2 and 4 months of age were examined with slit lamp biomicroscopy. Fixed eyes were subjected to histologic analysis. On gross examination, lenses of all rats appeared clear and free of any light scatter (Fig. 4A). Slit lamp analysis of the eyes of these rats showed no evidence of opacities at 2 and 4 months of age (Fig. 4B); these observations were confirmed in isolated lenses from *Slc16a12*^{TKO} rats (Fig. 4C). Histologic examination of eyes from these animals showed that the morphology of fiber cells in the equatorial region of the lens was similar in *Slc16a12*^{WT} and *Slc16a12*^{TKO} lenses (Fig. 4D). Fiber cells are arranged with a very high level of long-range order, which is essential for clarity. Some knockouts have shown a loss of this tissue level organization, as demonstrated by scanning electron microscopy (SEM), but with only the subtlest of light scatter and without obvious histologic changes.[19,20] To ensure that we were not missing a significant structural phenotype, lenses from *Slc16a12*^{TKO} rats were examined by SEM. A lower magnification overview (Fig. 4E) shows that the absence of MCT12 protein results in no significant change in the tissue level organization of fiber cells. The exceptional degree of alignment of fiber cells is apparent and is not distinguishable from the wild-type lens (not shown). Similarly, a higher magnification view (Fig. 4F) reveals no obvious changes in the structure of the fiber cells relative to wild-type lenses (not shown). Taken together, these data indicate that complete loss of *Slc16a12* does not induce cataract formation in a rat model up to age 4 months.

No significant differences were observed in the histology of the corneal epithelium (arrows) or the corneal endothelium (arrowheads) of *Slc16a12*^{WT} and *Slc16a12*^{TKO} rats (Supplementary Fig. S2, http://www.iovs.org/lookup/suppl/doi:10.1167/iovs.10-6579/-/DCSupplemental), indicating that the total loss of *Slc16a12* does not lead to microcornea in the rat, a feature that cosegregated with juvenile autosomal dominant cataract and the human truncation mutation.[1]

MCT12 Truncation Mutant Is Not Trafficked to the Plasma Membrane

Given that the *Slc16a12*^{TKO} rats did not have a lens phenotype, we explored the possibility that the mutant protein was mis-

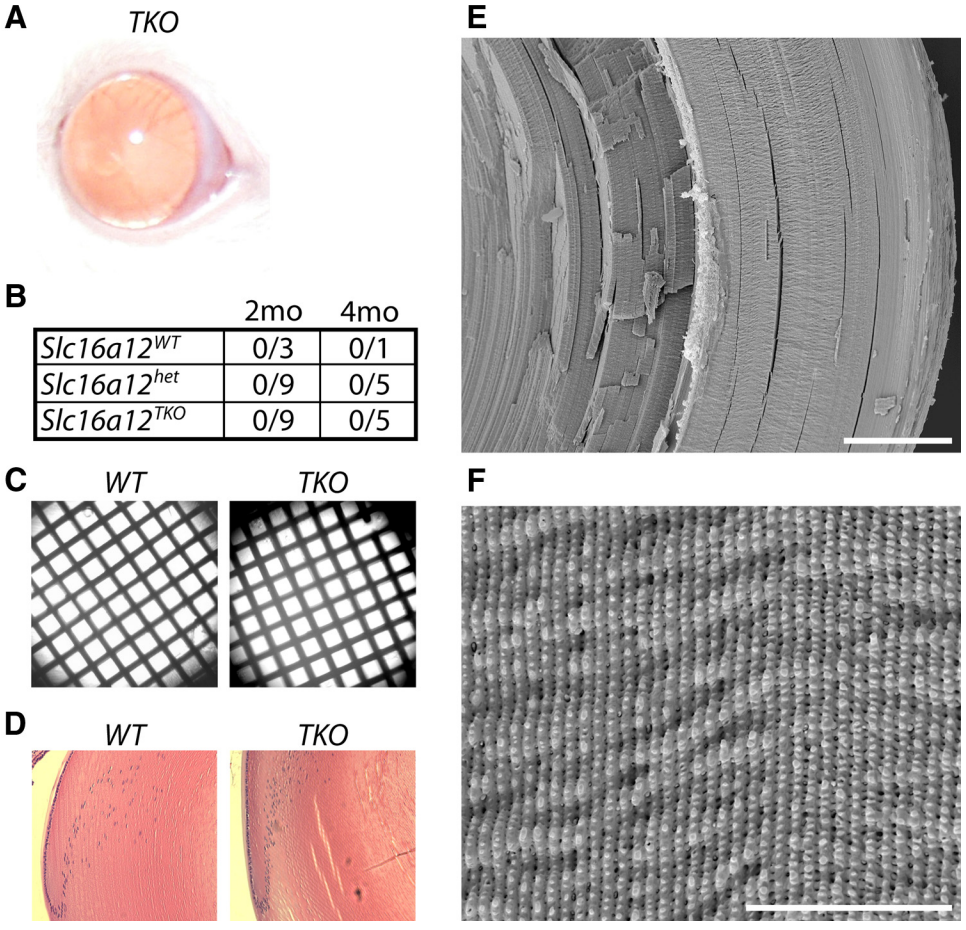

Figure 4. *Slc16a12*^{TKO} rats do not develop cataracts. (**A**) The eyes of *Slc16a12*^{TKO} rats were dilated with tropicamide, and a picture of the eye was taken with a digital camera before slit lamp examination. (**B**) Results of the slit lamp analysis. (**C**) Light microscopy was performed to assess clarity of the lens in *Slc16a12*^{WT} and *Slc16a12*^{TKO} eyes. Lenses were placed on 300 mesh square copper grids, and the ability to clearly see the square grid pattern was an indicator of lack of lens defect. (**D**) Hematoxylin and eosin staining of the equatorial region of *Slc16a12*^{WT} and *Slc16a12*^{TKO} rat lenses. (**E**) SEM was used to determine whether the null phenotype resulted in a loss of either lens tissue-level architecture or fiber cell shape, both of which are critical to optical clarity. Low-magnification overview of approximately 80% of a lens radius, spanning from the equatorial surface (*right*) toward the nucleus (*left*). Several hundred flat, ribbon-like fiber cells are seen edge on, arcing from left to right across the image. Artifacts of tissue preparation are evident as fissures or cracks between layers (*arrow*). (**F**) A higher magnification view of the outer lens, showing the well-aligned lateral edges of approximately 40 fiber cells arcing top to bottom. The lateral edges are decorated with dozens of small knob-like protrusions. Scale bars, 200 μm.

folded and not trafficked to the plasma membrane. To investigate this possibility, we generated expression vectors of truncated MCT12 designed to mimic expression of the $MCT12_{Q215X}$ mutant (MCT12:214Δ). MCT12:214Δ was expressed as either GFP or mCherry fusion protein in HEK-293 cells. As shown (Figs. 1A, 2B), full-length MCT12-GFP was primarily localized to the plasma membrane, as indicated by GFP labeling at the cell-cell borders, filopodia, and lamellipodia. In contrast, when we expressed MCT12:214Δ-GFP in HEK-293 cells, the fusion protein was retained in the ER, as demonstrated by its colocalization with the ER marker glucose-regulated protein, 78 kDa (GRP78, BIP) (Fig. 5A). The full-length MCT12 fusion did not colocalize with GRP78. A similar distribution of MCT12-GFP and MCT12:214Δ-GFP was observed in the HLE-B3 lens epithelial cell line, similar to that in HEK-293 cells (Supplementary Figs. S3A, S3B, http://www.iovs.org/lookup/suppl/doi:10.1167/iovs.10-6579/-/DCSupplemental), indicating that the ER retention of MCT12:214Δ-GFP is not cell-type specific.

Cell surface biotinylation followed by avidin precipitation was performed to further assess the trafficking of MCT12:214Δ-GFP to the plasma membrane. Blots of cell lysates and avidin precipitates showed that MCT12-GFP was enriched in the avidin-precipitated fraction (Fig. 5B), whereas MCT12:214Δ-GFP was barely detected in this fraction. The small amount that could be detected in the avidin-precipitated fraction could be attributed to a very small amount of MCT12:214Δ-GFP reaching the surface or to incomplete inactivation of the biotinylation reaction. Regardless, the ratio of precipitated to soluble MCT12-GFP was orders of magnitude greater than that of MCT12:214Δ-GFP. As a control, the blots were reprobed with CD147 antibody, which showed that the fully glycosylated form of CD147 was enriched to a similar degree in the biotinylated fractions of both cell lines. This indicates that the difference in the biotinylation of MCT12-GFP compared with MCT12:214Δ-GFP was not caused by variation in biotinylation in the different cell lines. The difference in expression levels between MCT12-GFP and MCT12:214Δ-GFP could not be accounted for by differential detergent solubility of the fusion proteins because both proteins were distributed to a similar degree between the detergent-soluble and the detergent-insoluble fractions (Supplementary Fig. S3B, http://www.iovs.org/lookup/suppl/doi:10.1167/iovs.10-6579/-/DCSupplemental). Furthermore, mRNA levels expressed from the transfected vectors were roughly equivalent (Fig. 5C).

Differences in the levels of MCT12-GFP and MCT12:214Δ-GFP could be attributed to degradation of the misfolded protein. To test this possibility, we treated cells with lactacystin, a proteasome inhibitor. Lactacystin treatment increased MCT12:214Δ-GFP levels approximately 5.6-fold, whereas MCT12-GFP levels increased by only 0.5-fold (Figs. 6A, 6B). This difference was statistically significant ($P < 0.004$). Degradation of MCT12:214Δ by the proteasome pathway indicates that the truncated protein is a target of the ER-associated degradation pathway and therefore is likely misfolded.

To determine whether trafficking of full-length MCT12 to the plasma membrane could be disrupted by coexpression with MCT12:214Δ, as would be the case if $MCT12_{Q215X}$ behaved as a dominant-negative, stable HEK-293:MCT12-GFP, cells were transiently transfected with mCherry-MCT12:214Δ. In cells expressing both full-length and truncated proteins, MCT12-GFP was detected at the plasma membrane but mCherry-MCT12:214Δ remained intracellular (Fig. 6C), indicating that expression and trafficking of the full-length protein were not disrupted by the truncated protein.

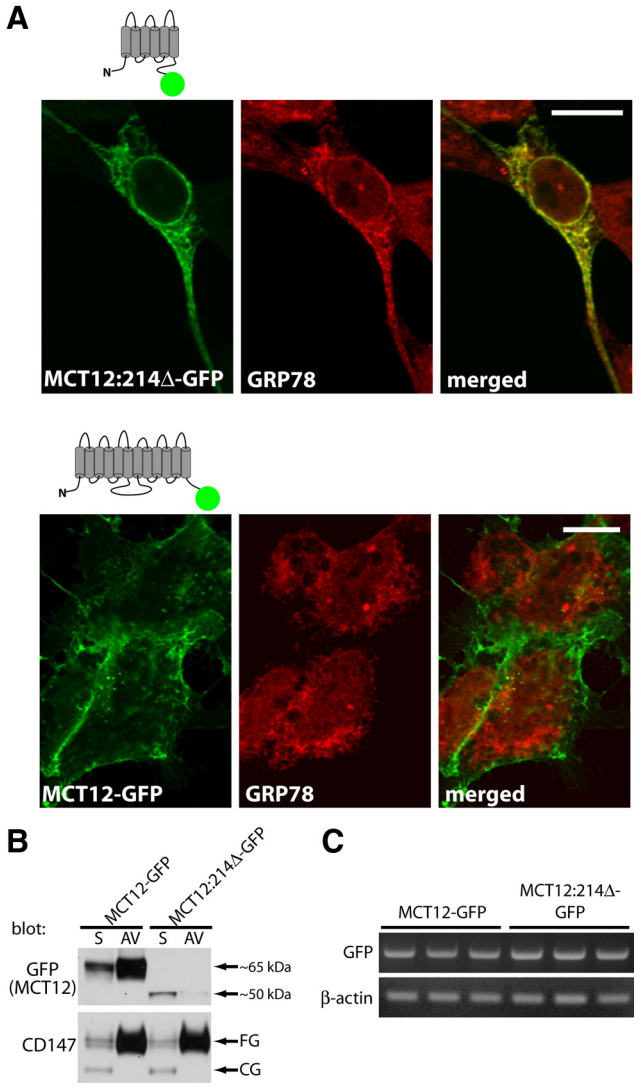

FIGURE 5. MCT12:214Δ is retained in the ER. (**A**) HEK-293 cells transiently transfected with vectors expressing either MCT12:214Δ-GFP (*upper*) or MCT12-GFP (*lower*) were immunostained for GRP78 (*red*). Scale bars, 10 μm. (**B**) HEK-293 cells transiently transfected with vectors expressing either MCT12-GFP or MCT12:214Δ-GFP were cell-surface biotinylated 48 hours after transfection. Biotinylated proteins were precipitated from cell lysates with streptavidin-agarose beads. Soluble (S) and avidin-precipitated (Av) fractions were run by SDS-PAGE and subjected to Western blot analysis, and the blots were probed for GFP and CD147. (**C**) To determine whether differences in protein levels between MCT12-GFP and MCT12:214Δ-GFP were due to differences in mRNA levels, mRNA was extracted from HEK-293 cells transiently transfected with either MCT12-GFP or MCT12:214Δ-GFP 48 hours after transfection, and cDNA was prepared. PCR was performed for GFP to unify amplification from both constructs and β-actin as a control.

ER Retention of Truncated MCT12 Is Not MCT12 Specific

To determine whether the retention of truncated MCT12:214Δ in the ER was specific for MCT12 or a phenomenon of truncated MCTs in general, we generated a truncation of MCT4 within the large intracellular loop between transmembrane domains 6 and 7 and expressed it as a GFP fusion (MCT4:207Δ-GFP) in HEK-293 cells. Although normal MCT4 is trafficked to the plasma membrane[21] (Fig. 7A), MCT4:207Δ-GFP was retained in the ER (Fig. 7B). This finding suggests that premature

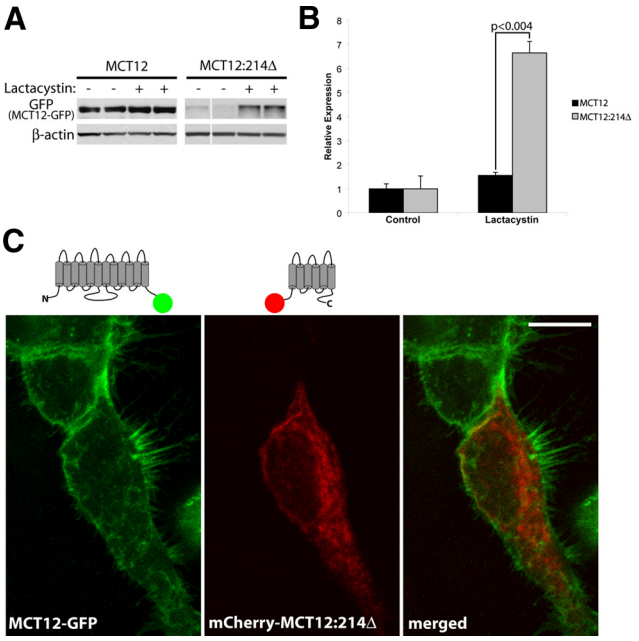

Figure 6. MCT12:214Δ is degraded by proteasomes and is not dominant-negative. Forty hours after transfection with vectors expressing either MCT12-GFP or MCT12:214Δ-GFP, HEK-293 cells were treated with 10 μM lactacystin for 8.5 hours. Note: MCT12-GFP and MCT12:214Δ-GFP are actually of different molecular weights, as shown in Figure 5B. Western blot analysis (**A**) was quantitated (**B**), and the relative levels of MCT12-GFP and MCT12:214Δ-GFP were determined in control and lactacystin-treated cells as normalized to β-actin signal. Error bars are $\pm$ SD ($n = 3$). (**C**) To determine whether MCT12:214Δ disrupts full-length MCT12 localization, HEK-293:MCT12-GFP cells were transiently transfected with mCherry-MCT12:214Δ. Cells were fixed 48 hours after transfection and imaged by confocal microscopy. Illustrations specify fusion protein and type of tag. Scale bar, 10 μm.

termination of any MCT is likely to cause ER retention because of protein misfolding.

Discussion

SLC16A12 was identified by Halestrap and Visser[2] through searching the human genomic and EST databases; however, nothing is known about the properties or function of the protein. Recently, it was discovered that patients with a nonsense mutation in *SLC16A12* develop juvenile cataract with a dominant inheritance pattern.[1] In this study, we investigated potential mechanisms by which the mutation in exon 6 (c.643C>T) of *SLC16A12* could lead to cataract formation. We focused on two possibilities: haploinsufficiency caused by reduced levels of the normal transporter molecules or a direct effect of the truncated protein. The evidence presented here suggests that $MCT12_{Q215X}$ is retained in the ER and that protein misfolding and trafficking defects, rather than haploinsufficiency, are the underlying cause of cataract formation.

MCTs have been localized to plasma and mitochondrial membranes; therefore, in the present study, we used cell lines expressing an MCT12-GFP fusion protein to assess the subcellular distribution of the protein.[2,22] In both HEK-293 and HLE-B3 cells, MCT12 was trafficked to the plasma membrane. Moreover, we demonstrated for the first time that maturation and trafficking of MCT12 to the plasma membrane required the accessory protein CD147. These studies reveal that MCT12, like MCT1, MCT3, and MCT4, requires assembly with CD147 for stability and cell surface expression. MCT12 was detected in the plasma membrane of lens epithelial cells and in differentiating and secondary fiber cells as early as P1 in the mouse. The temporal and spatial expression of MCT12 in lens epithelium and secondary fiber cells was consistent with corticonuclear cataract observed in patients with *SLC16A12*(c.643C>T) mutations.

Mutations in facilitated solute transporters can cause disease because of alterations in expression, trafficking, or functional activity. To determine the fate of the $MCT12_{Q215X}$ protein produced from the *SLC16A12* cataract-associated mutation, we expressed a mimic (MCT12:214Δ-GFP) in HEK-293 cells. The truncated MCT12, composed only of the first six transmembrane domains, was retained in the ER (Fig. 5) and was degraded by the proteasome pathway, indicative of misfolding (Fig. 6). Although the crystal structures of MCT family members have not been determined, molecular modeling based on the structure of the *Escherichia coli* homolog lactose permease (LacY) transporter has been performed.[23,24] Models of the tertiary structures of MCT1, MCT8, and LacY predict interactions of the first and second halves of MCT by close associations between transmembrane domains 5–8 and 2–11.[2,9,25] The transmembrane domains of MCTs are well conserved; thus, a similar arrangement likely exists for MCT12. Therefore, any mutation that would cause such an early premature termination of an MCT would likely lead to misfolding. Indeed, performing a similar truncation of MCT4 also led to retention of the resultant protein in the ER (Fig. 7). Expression of the truncated protein does not affect expression of the wild-type (Fig. 6C); therefore, $MCT12_{Q215X}$ does not function as dominant-negative. There is considerable overlap of transport properties among different gene families; hence, it is rare that haploinsufficiency of a solute transporter results in a phenotype.[26] Haploinsufficiency of the connexins *Gja3* and *Gja8* does not result in cataract formation in mice because the heterozygotes lack a detectable phenotype. To address the possibility that cataract formation in patients with the *SLC16A12* c.643C>T mutation resulted from haploinsufficiency, we examined the eyes of the $Slc16a12^{TKO}$ rat. The lack of cataract phenotype in either the heterozygote or the homozygote rat would not immediately support a model of haploinsufficiency. Further, there was no evidence of cataract formation in *Bsg*-deficient (CD147) mice[27] (Judith Ochrieter, personal communication, 2011). It is ex-

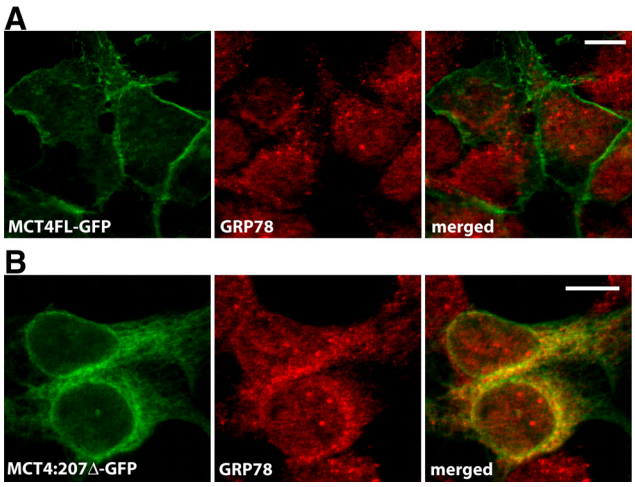

Figure 7. Truncated MCT4 behaves like MCT12:214Δ. To determine whether defective trafficking of MCT12:214Δ was specific to MCT12, we generated a similar truncation of MCT4, MCT4:207Δ-GFP. Cells were fixed 48 hours after transfection and were stained for GRP78 (*red*). MCT4-GFP (**A**) is present predominantly at the cell surface, whereas MCT4:207Δ-GFP (**B**) is predominantly retained in the ER. Scale bars, 10 μm.

pected that these mice would have a loss of MCT1, MCT4, and MCT12 activity in the lens because the accessory protein is required for maturation of the transporters.[12]

The genetic robustness of the *Slc16a12*^{TKO} rat may be attributed to genetic buffering or functional complementation or redundancy. The observed increased expression of *Slc16a10* mRNA in *Slc16a12*^{TKO} lenses may support this explanation if both transporters have similar substrate specificities. We know that MCT10 transports aromatic amino acids[28] and thyroid hormone,[4] but the transported substrate of MCT12 is not yet known. This information would shed light on the possibility that functional redundancy may be responsible for the lack of a phenotype. Because antibodies that recognize rat MCT10 are not available, confirmation about whether the observed increase in *Slc16a10* transcripts in the lenses of *Slc16a12*^{TKO} rats also leads to an increase in functional MCT10 protein awaits experimental testing. Furthermore, the genetic background of the rat strain used in these studies may have inherent resistance to cataract formation; alternatively, extrinsic environmental factors could also play a role in cataractogenesis in humans to which our animal model was not exposed.[29]

Knocking out genes often does not result in a phenotype whereas knocking in the mutant gene does because of a negative gain of function of the mutant protein. For example, a knockout model of connexin 50 has a slowly developing cataract, whereas the mutation mimicking human cataract-associated phenotype displays a much more severe cataract.[30,31] Additionally, mutations in SLC16A2 that affect trafficking of MCT8 to the plasma membrane result in a more severe phenotype than those that affect transport activity. Similar to our findings with *Slc16a12*^{TKO} rats, *Slc16a2* knockout mice show no signs of the neurologic abnormalities observed in patients.[32,33] Based on the cell-based assays with MCT12:214Δ-GFP and the lack of phenotypes in the *Slc16a12*^{TKO} rats and *Bsg* knockout mice, we would expect that a knock-in of the mutated allele would be the only mechanism to accurately assess the development of the *SLC16A12*(c.643C>T)–associated cataract.

MCT12 was detected in the equatorial lens epithelial cells, which differentiate into lens fiber cells. The transition from an epithelial cell to a mature fiber cell necessitates a large increase in protein and lipid synthesis and a degradation of intracellular organelles. These cells already undergo an unfolded protein response, and it is likely that cells in this region of the lens would be hypersensitive to additional stress caused by a mutated, misfolded protein.[34] Expression of the MCT12$_{Q215X}$ mutant protein in the equatorial region of the lens could result in excessive ER stress, which is known to cause cataract.[35–37] The juvenile corticonuclear cataract observed in patients with *SLC16A12*(c.643C>T) mutations would be expected if the temporal and spatial expression of MCT12 observed in the mouse lens is recapitulated in the human lens.

Overall, our findings suggest that cataract formation in patients with the c.643C>T mutation in *SLC16A12* is due to a defect in protein folding and trafficking causing ER stress in the differentiating and secondary lens fiber cells. The transporter knockout model provided a valuable tool to assess the contribution of individual transporters to lens transparency. Future studies with humanized rat models will provide further insight into how specific mutations lead to cataract formation, thereby providing valuable models for determining whether juvenile cataracts arising from defects in protein trafficking can be treated pharmacologically rather than surgically.

References

1. Kloeckener-Gruissem B, Vandekerckhove K, Nurnberg G, et al. Mutation of solute carrier SLC16A12 associates with a syndrome combining juvenile cataract with microcornea and renal glucosuria. *Am J Human Genet.* 2008;82:772–779.
2. Halestrap AP, Meredith D. The SLC16 gene family from monocarboxylate transporters (MCTs) to aromatic amino acid transporters and beyond. *Pflugers Archiv Eur J Physiol.* 2004;447:619–628.
3. Grollman EF, Philp NJ, McPhie P, Ward RD, Sauer B. Determination of transport kinetics of chick MCT3 monocarboxylate transporter from retinal pigment epithelium by expression in genetically modified yeast. *Biochemistry.* 2000;39:9351–9357.
4. Friesema EC, Jansen J, Jachtenberg JW, Visser WE, Kester MH, Visser TJ. Effective cellular uptake and efflux of thyroid hormone by human monocarboxylate transporter 10. *Mol Endocrinol.* 2008;22:1357–1369.
5. Illig T, Gieger C, Zhai G, et al. A genome-wide perspective of genetic variation in human metabolism. *Nat Genet.* 2010;42:137–141.
6. Kolz M, Johnson T, Sanna S, et al. Meta-analysis of 28,141 individuals identifies common variants within five new loci that influence uric acid concentrations. *PLoS Genet.* 2009;5:e1000504.
7. Ramadan T, Camargo SM, Herzog B, Bordin M, Pos KM, Verrey F. Recycling of aromatic amino acids via TAT1 allows efflux of neutral amino acids via LAT2–4F2hc exchanger. *Pflugers Arch.* 2007; 454:507–516.
8. Ramadan T, Camargo SM, Summa V, et al. Basolateral aromatic amino acid transporter TAT1 (Slc16a10) functions as an efflux pathway. *J Cell Physiol.* 2006;206:771–779.
9. Wilson MC, Meredith D, Bunnun C, Sessions RB, Halestrap AP. Studies on the DIDS-binding site of monocarboxylate transporter 1 suggest a homology model of the open conformation and a plausible translocation cycle. *J Biol Chem.* 2009;284:20011–20021.
10. Kirk P, Wilson MC, Heddle C, Brown MH, Barclay AN, Halestrap AP. CD147 is tightly associated with lactate transporters MCT1 and MCT4 and facilitates their cell surface expression. *EMBO J.* 2000; 19:3896–3904.
11. Wilson MC, Meredith D, Halestrap AP. Fluorescence resonance energy transfer studies on the interaction between the lactate transporter MCT1 and CD147 provide information on the topology and stoichiometry of the complex in situ. *J Biol Chem.* 2002;277:3666–3672.
12. Philp NJ, Ochrietor JD, Rudoy C, Muramatsu T, Linser PJ. Loss of MCT1, MCT3, and MCT4 expression in the retinal pigment epithelium and neural retina of the 5A11/basigin-null mouse. *Invest Ophthalmol Vis Sci.* 2003;44:1305–1311.
13. Gallagher SM, Castorino JJ, Wang D, Philp NJ. Monocarboxylate transporter 4 regulates maturation and trafficking of CD147 to the plasma membrane in the metastatic breast cancer cell line MDA-MB-231. *Cancer Res.* 2007;67:4182–4189.
14. Wilson MC, Meredith D, Fox JE, Manoharan C, Davies AJ, Halestrap AP. Basigin (CD147) is the target for organomercurial inhibition of monocarboxylate transporter isoforms 1 and 4: the ancillary protein for the insensitive MCT2 is EMBIGIN (gp70). *J Biol Chem.* 2005;280:27213–27221.
15. Hejtmancik JF. Congenital cataracts and their molecular genetics. *Semin Cell Dev Biol.* 2008;19:134–149.
16. Lu B, Geurts AM, Poirier C, et al. Generation of rat mutants using a coat color-tagged Sleeping Beauty transposon system. *Mamm Genome.* 2007;18:338–346.
17. Philp NJ, Wang D, Yoon H, Hjelmeland LM. Polarized expression of monocarboxylate transporters in human retinal pigment epithelium and ARPE-19 cells. *Invest Ophthalmol Vis Sci.* 2003;44:1716–1721.
18. Deora AA, Philp N, Hu J, Bok D, Rodriguez-Boulan E. Mechanisms regulating tissue-specific polarity of monocarboxylate transporters and their chaperone CD147 in kidney and retinal epithelia. *Proc Natl Acad Sci U S A.* 2005;102:16245–16250.
19. Alizadeh A, Clark JI, Seeberger T, et al. Targeted genomic deletion of the lens-specific intermediate filament protein CP49. *Invest Ophthalmol Vis Sci.* 2002;43:3722–3727.
20. Yoon KH, Blankenship T, Shibata B, FitzGerald PG. Resisting the effects of aging: a function for the fiber cell beaded filament. *Invest Ophthalmol Vis Sci.* 2008;49:1030–1036.

21. Castorino JJ, Deborde S, Deora A, et al. Basolateral sorting signals regulating tissue-specific polarity of heteromeric monocarboxylate transporters in epithelia. *Traffic.* 2011;12:483–498.
22. Brooks GA, Hashimoto T. Investigation of the lactate shuttle in skeletal muscle mitochondria. *J Physiol.* 2007;584:705–706; author reply 707–708.
23. Abramson J, Smirnova I, Kasho V, Verner G, Kaback HR, Iwata S. Structure and mechanism of the lactose permease of *Escherichia coli*. *Science.* 2003;301:610–615.
24. Galic S, Schneider HP, Broer A, Deitmer JW, Broer S. The loop between helix 4 and helix 5 in the monocarboxylate transporter MCT1 is important for substrate selection and protein stability. *Biochem J.* 2003;376:413–422.
25. van der Deure WM, Peeters RP, Visser TJ. Molecular aspects of thyroid hormone transporters, including MCT8, MCT10, and OATPs, and the effects of genetic variation in these transporters. *J Mol Endocrinol.* 2010;44:1–11.
26. DeGorter MK, Kim RB. Use of transgenic and knockout mouse models to assess solute carrier transporter function. *Clin Pharmacol Ther.* 2011;89:612–616.
27. Naruhashi K, Kadomatsu K, Igakura T, et al. Abnormalities of sensory and memory functions in mice lacking *Bsg* gene. *Biochem Biophys Res Commun.* 1997;236:733–737.
28. Kim DK, Kanai Y, Chairoungdua A, Matsuo H, Cha SH, Endou H. Expression cloning of a Na+-independent aromatic amino acid transporter with structural similarity to H+/monocarboxylate transporters. *J Biol Chem.* 2001;276:17221–17228.
29. Barbaric I, Miller G, Dear TN. Appearances can be deceiving: phenotypes of knockout mice. *Brief Funct Genomic Proteomic.* 2007;6:91–103.
30. Xia CH, Cheng C, Huang Q, et al. Absence of alpha3 (Cx46) and alpha8 (Cx50) connexins leads to cataracts by affecting lens inner fiber cells. *Exp Eye Res.* 2006;83:688–696.
31. DeRosa AM, Mese G, Li L, et al. The cataract causing Cx50–S50P mutant inhibits Cx43 and intercellular communication in the lens epithelium. *Exp Cell Res.* 2009;315:1063–1075.
32. Trajkovic M, Visser TJ, Mittag J, et al. Abnormal thyroid hormone metabolism in mice lacking the monocarboxylate transporter 8. *J Clin Invest.* 2007;117:627–635.
33. Di Cosmo C, Liao XH, Dumitrescu AM, Philp NJ, Weiss RE, Refetoff S. Mice deficient in MCT8 reveal a mechanism regulating thyroid hormone secretion. *J Clin Invest.* 2010;120:3377–3388.
34. Firtina Z, Duncan MK. Unfolded Protein Response (UPR) is activated during normal lens development. *Gene Expr Patterns.* 2011;11:135–143.
35. Watson GW, Andley UP. Activation of the unfolded protein response by a cataract-associated alphaA-crystallin mutation. *Biochem Biophys Res Commun.* 2010;401:192–196.
36. Mulhern ML, Madson CJ, Danford A, Ikesugi K, Kador PF, Shinohara T. The unfolded protein response in lens epithelial cells from galactosemic rat lenses. *Invest Ophthalmol Vis Sci.* 2006;47:3951–3959.
37. Firtina Z, Danysh BP, Bai X, Gould DB, Kobayashi T, Duncan MK. Abnormal expression of collagen IV in lens activates unfolded protein response resulting in cataract. *J Biol Chem.* 2009;284:35872–35884.